Cancer Letters 430 (2018) 201–214

Contents lists available at ScienceDirect

Cancer Letters

journal homepage: www.elsevier.com/locate/canlet

Original Articles

CD146 mediates an E-cadherin-to-N-cadherin switch during TGF-β signaling-induced epithelial-mesenchymal transition

Yanbin Ma[a,b,1], Haofeng Zhang[c,1], Chaoliang Xiong[a,b], Zheng Liu[a], Qingji Xu[a,b], Jing Feng[a], Jun Zhang[c,*], Zhaoqing Wang[a,**], Xiyun Yan[a,b,***]

[a] Key Laboratory of Protein and Peptide Pharmaceuticals, Institute of Biophysics, Chinese Academy of Sciences, Beijing, 100101, China
[b] University of Chinese Academy of Sciences, Beijing, 100049, China
[c] Obstetrics and Gynecology Medical Center of Severe Cardiovascular Disease of Beijing, Anzhen Hospital, Capital Medical University, Beijing, 100029, China

ABSTRACT

Cadherin switch is an initiating factor of epithelial-mesenchymal transition (EMT) and is intimately correlated with cancer metastatic potential; however, its underlying mechanisms remain unclear. Here, using a transforming growth factor-β (TGF-β)-induced EMT model, we provide explicit evidence that CD146, with elevated expression and activity in a variety of cancers, is a key factor involved in the cadherin switch. We show that CD146 can be induced by TGF-β signaling. Moreover, CD146 expression is positively correlated with the activation levels of STAT3/Twist and ERK pathways. Transcriptional response of the CD146/STAT3/Twist cascade inhibits E-cadherin expression, whereas the CD146/ERK cascade enhances N-cadherin expression. CD146 overexpression also significantly promotes EMT in both mouse embryonic fibroblasts (MEFs) and ovarian cancer cells. Clinically, ovarian cancer patients with detectable CD146 expression had a significantly lower survival rate than that of patients without CD146 expression. Furthermore, CD146-deficient MEFs exhibited decreased motility as a result of reversion in this cadherin switch, strongly suggesting that targeting CD146 is a potential strategy for cancer treatment. Therefore, CD146-mediated regulation of the E-cadherin-to-N-cadherin switch provides an insight into the general mechanisms of EMT as well as cancer metastasis.

1. Introduction

Loss or reduction of E-cadherin expression and induction of N-cadherin expression is known as the "E-cadherin-to-N-cadherin switch" [1]. E− and N-cadherin are members of the classical cadherin family that play an important role in regulating cellular morphology [2]. E-cadherin is expressed by most normal epithelial tissues, whereas N-cadherin is typically expressed by mesenchymal cells [3–5]. Many cancer cells possess the characteristic of this cadherin switch, which initiates a process referred to as EMT [6–8]. However, the mechanism underlying this cadherin switch remains unclear.

EMT is a common feature of both embryonic development and tumor metastasis [9,10]. It leads to loosening of intercellular junctions, and consequently allows cells to overcome cell–cell contact inhibition of migration [11,12]. Thus, tumor cells undergoing EMT transform from a quiescent to a metastatic phenotype [11,13]. Metastasis is responsible for around 90% of cancer-associated mortality. Therefore, elaborating the EMT process will facilitate better understanding of the mechanism underlying cancer metastasis [14,15], a process which remains one of the most poorly understood components in cancer pathogenesis.

The cadherin switch can be induced by numerous environmental signals that activate an array of EMT transcriptional factors (EMT-TFs), including Snail1, Snail2 (Slug), Zeb, and Twist. As transcriptional EMT inducers, these EMT-TFs directly bind to the promoter regions of a plethora of epithelial marker genes such as E-cadherin, to repress their

Abbreviations: E-cadherin, epithelial cadherin; N-cadherin, neuronal cadherin; EMT, epithelial-mesenchymal transition; EMT-TF, EMT transcriptional factor; TGF-β, transforming growth factor-β; BMP, bone morphogenetic protein; MEF, mouse embryonic fibroblast; WT, wild type; KO, knockout; OE, overexpression; ERK, extracellular regulated protein kinase; STAT3, signal transducers and activators of transcription; MAPKs, mitogen activated protein kinase; FGF, fibroblast growth factor; VEGF, vascular endothelial growth factor; PDGF, platelet-derived growth factor; R-SMAD, receptor-activated SMAD; IHC, immunohistochemistry

* Corresponding author.
** Corresponding author. Key Laboratory of Protein and Peptide Pharmaceuticals, Institute of Biophysics, Chinese Academy of Sciences, Beijing, 100101, China.
*** Corresponding author.
E-mail addresses: drzhangj@outlook.com (J. Zhang), clairezqwang@163.com (Z. Wang), yanxy@ibp.ac.cn (X. Yan).
[1] These authors contributed equally to this work.

https://doi.org/10.1016/j.canlet.2018.05.016
Received 27 March 2018; Received in revised form 11 May 2018; Accepted 12 May 2018

expression [16–19]. N-cadherin is reported to be upregulated by TGF-β signaling [20,21].

TGF-β1 has been identified as the most potent factor that can independently induce EMT and activate EMT-TFs in various types of cancer cells [22–24]. The TGF-β superfamily comprises TGF-βs, bone morphogenetic proteins (BMPs), activins, and related proteins [25–27]. In vertebrates, the intracellular effectors of TGF-β signaling are SMAD proteins. It is now known that co-activation of both SMAD-dependent canonical and SMAD-independent non-canonical pathways is needed for the initiation and completion of TGF-β-induced EMT [28,29].

Ovarian cancer has a poor prognosis, and it remains the leading cause of mortality among gynecological cancers because the majority of patients have progressed to advanced stages by the time of their first clinical visit [30–32]. However, a lack of reliable diagnostic markers and potential therapeutic targets continues to restrict both the successful detection of ovarian cancer in early stages and the effective treatment of this disease at later stages [33].

CD146 is an inducible signaling receptor that can drive various cancers to progress into malignant metastasis [34–36]. The expression and activity of CD146 are elevated in a variety of cancers, but its mechanisms are not exactly understood [34]. Artificial overexpression of CD146 alone is sufficient to induce EMT progression in the human breast cancer cell line, MCF-7, which does not express CD146 endogenously [37]. Given that forced overexpression of CD146 induces EMT progression in $CD146^-$ MCF-7 cells [37], we speculated whether CD146 is inducible in CD146 positive cells, what factors can induce CD146 upregulation, and how CD146 drives $CD146^+$ cells progression into EMT.

Here, using a TGF-β-induced EMT model, we show that CD146 can be induced by TGF-β signaling, and that CD146 is required for cells to become fully mesenchymal. An inability to complete the EMT in the absence of CD146 appears to involve a reversal of the E-to N-cadherin switch.

2. Materials and methods

2.1. Antibodies

AA1 (1:1000) is a murine anti-CD146 monoclonal antibody generated in our laboratory; this antibody recognizes the first V domain in the extracellular region of CD146.Additional information for all commercial antibodies is as follows: The anti-SMAD7 antibody (25840-1-AP) was purchased from Proteintech (Chicago, USA). The anti-Twist antibody (sc-81417) was purchased from Santa Cruz Biotechnology (Dallas,USA). The anti-JNK (1:1000, #9252 S), anti-phospho-JNK (1:1000, #9251 S), anti-ERK (1:1000, #9107), anti-phospho-ERK (1:1000, #4370), anti-p38 (1:1000, #9107), anti-phospho-p38 (1:1000, #4511), anti-Snail1 (1:1000, #3879),anti-Slug (1:1000, #9585), anti-Zeb1 (1:1000, #3396), anti-phospho-SMAD1/P-SMAD5 (1:1000, #9516), anti-phospho-SMAD2/P-SMAD3 (1:1000, #8828), anti-NF-κB/p65 (1:1000, #8242), and anti-phospho-NF-κB/p65 (1:1000, #3033) antibodies and Alexa Fluor 488 Phalloidin (1:2000, 8878 S)were from Cell Signaling Technology (Boston, USA). Anti-STAT3 (1:3000, 10253-2-AP) was from Proteintech (Chicago, USA). The anti-CD146 (ab75769), anti-phospho-STAT3 (1:3000, phospho Y705, ab76315), anti-SMAD1 (1:2000, ab33902), anti-SMAD2 (1:2000, ab33875), anti-SMAD3 (1:2000, ab40854), anti-SMAD4 (1:2000, ab40759), anti-SMAD5 (1:2000, ab151267), anti-SMAD6 (1:2000, ab13727), anti-N-cadherin (1:2000, ab18203), and anti-E-cadherin (1:2000, ab76055) antibodies were from Abcam (Cambridge, USA).

2.2. Reagents

All chemicals were purchased from Sigma (Darmstadt, Germany). All cell culture media were from Gibco (Waltham, USA) and all transfection reagents were from Invitrogen (Carlsbad, USA). Protease inhibitor and PhosSTOP (phosphatase inhibitor cocktail) were from Roche (Basel, Switzerland). The Dual-Luciferase System (E1910) was from Promega (Madison, USA). Recombinant human/rhesus/canine TGF-β1 (10804-HNAC), rat/mouse TGF-β1 (80116-RNAE), and human/mouse/rat/rhesus/canine BMP-4 proteins (10426-HNAE), were from Sino Biological Inc. (Beijing China). The STAT3 inhibitor (NSC74859) and ERK inhibitor (U0126) were from MCE Biological Inc. (Monmouth Junction, USA).

2.3. Cell lines with culture conditions and treatments

All cell lines were obtained from ATCC (Manassas, USA) and were authenticated by single nucleotide polymorphism testing and mycoplasma contamination testing. The mouse embryonic fibroblast (MEF) cell line (CRL-2752), CD146 knockout MEFs, and CD146 over-expressing MEFs were maintained in Eagle's minimum essential medium supplemented with 10% fetal bovine serum (FBS). The human ovarian cancer cell line SKOV3 (HTB-77) was maintained in McCoy's 5a medium supplemented with 10% FBS. After overnight depletion of serum from the culture medium, cells were treated with TGF-β1 or BMP-4 for the indicated times at 37 °C.

2.4. Establishment of CD146 knockout mouse embryonic fibroblasts

Wild type mouse embryonic fibroblasts ($CD146^{WT}$MEFs) were obtained from ATCC (CRL-2752), and authenticated by single nucleotide polymorphism testing and mycoplasma contamination testing. They were maintained in Dulbecco's modified Eagle's Medium (DMEM) supplemented with 10% fetal bovine serum (FBS).

The mouse CD146 gene is located on the forward strand of the 9A5.1 region of chromosome 9, spanning approximately 8.14 kb with 5 transcripts. A transcript isoform containing 16 exons and encoding 648 amino acids (AA) (NP_075548.2) was chosen as the 'canonical' sequence for targeting (http://www.uniprot.org/uniprot/Q8R2Y2).

CD146 knockout ($CD146^{KO}$) MEF cell line was generated by Biocytogen (Beijing China). Briefly, exons 3–16 in the CD146 transcript isoform were replaced with a puromycin resistant gene cassette, using single guide CRISPR–Cas9 (Cas9/sgRNA)-mediated insertions or deletions(indels). The 1000bp of coding sequence upstream of CD146 exon 3 and the 1000bp of coding sequence downstream of CD146 exon were used as the 5′ and 3′homologous regions, respectively. Selection of resistant gene cassettes was determined by antibiotic titration and karyotyping experiments. The targeting vector included the 5′region, a CRISPR/Cas9-targeting site (a puromycin resistant gene cassette), the second CRISPR/Cas9-targeting site, and the 3′ region.

The Cas9/sgRNA targeting vector was transfected into the MEFs in the log-phase of grow that a concentration of 5 μg/10^6 cells. The transfectants were cultured at 37 °C in complete DMEM. After 24 h, the medium was replaced with complete DMEM containing 4 μg/mL puromycin and 400 μg/mL hygromycin B. The cells were cultured in this selection medium for 20 days, after which single cell colonies were transferred to a 48-well plate. When the cells reached full confluence, one half of each individual colony was collected for further identification, including PCR screening to confirm homologous recombination, indels analysis, genotyping, and immunoblotting using a specific antibody against CD146.

2.5. Design of single-guide RNAs and construction of sgRNA vector

To verify whether single nucleotide polymorphisms (SNPs) existed in these two targeting loci, exon 3 and exon 16 were amplified and sequenced for gRNA-mediated mutant sequence design (MSD) by PCR using four primers: CD146-N-MSD forward, 5′-CCT GGA CTT TGG AGG GCA GTA GTT G-3′; CD146-N-MSD reverse, 5′-GGG TTA CTC ACG GTT CTC CTCCTC T-3′; CD146-C-MSD forward, 5′-AGA GAG CAA AGG TGT GGT CAT CGT G-3′; CD146-C-MSD reverse, 5′-GAG GAA AAG ACA GAA

GTC CCC CAG C-3′.

Three sgRNAs targeting sequences on exon 3 were selected as follows: CD146-sgRNA-1, 5′-GAG CAA GCG ACC ACG GCT CC AGG-3′; CD146-sgRNA-2, 5′-GGA TCA CTA CGT TGA GCT TCA GG-3′; and CD146-sgRNA-3, 5′-ACG TAG TGA TCC TGG AGC CGT GG-3′. Three sgRNAs targeting sequences on exon 16 were selected as follows: CD146-sgRNA-4, 5′-CAA ATT CAC TCT TAC GAG TCG GG-3′; CD146-sgRNA-5, 5′-ACA AAT TCA CTC TTA CGA GTC GG-3′; CD146-sgRNA-6, 5′-TGA AGG AGA GCC ATC TCT TCT GG-3′. The sgRNA cloning vector TV-4G-EB was used for CRISPR/Cas9 construction. After detection of Cas9/sgRNA activity, sgRNA-3 and sgRNA-5 with relatively high activity were chosen for *cd146* gene targeting. The two pairs of primers used for PCR amplification of sgRNA-3 and sgRNA-5 were as follows: hmCD146-3-up, 5′-CACC GTA GTG ATC CTG GAG CCG-3′; hmCD146-3-down, 5′-AAAC CGG CTC CAG GAT CAC TAC-3′; hmCD146-5-up, 5′-CACC GAC AAA TTC ACT CTT ACG AGT-3′; hmCD146-5-down, 5′-AAAC ACT CGT AAG AGT GAA TTT GTC-3′.

2.6. Immunoblotting

Total cell lysates were collected using cell lysis buffer (Cell Signaling Technology, Boston, USA), supplemented with 1 mM PMSF and a protease inhibitor cocktail. The lysates were centrifuged and the supernatant was collected. Protein concentration was measured using a BCA protein Assay Kit (Pierce, Rockford, USA). Approximately 50 μg of cell lysate was subjected to sodium dodecyl sulfate-polyacrylamide gel electrophoresis (SDS-PAGE) and transferred to polyvinylidene difluoride (PVDF) membranes (Bio-Rad, Hercules, USA). Membranes were then blocked with 5% milk (in TBST) or 5% BSA (in TBST) for 30 min, incubated overnight at 4°C with the primary antibody, washed three times with TBST (5 min each), and incubated with the appropriate secondary antibody (5% milk in TBST) for 1 h. The signal was detected with an ECL reagent (Amersham, Little Chalfont, UK) following the manufacturer's instructions. Densitometry was performed using ImageJ software.

2.7. Establishment of CD146 overexpressing mouse embryonic fibroblasts

CD146 overexpressing ($CD146^{OE}$) MEFs were generated by SyngenTech (Beijing, China). CD146-expressing plasmids in a pHS-AVC-LW227 lentiviral vector were constructed using the following primers: HS-AVC-CD146 forward, 5′-GGA GCT GCT GGT GAA CTA TG-3′; and HS-AVC-CD146 reverse, 5′-TGC CAT GCA GAG ATA CCG TC-3′. This vector was packaged together with lentiviral particles in human embryonic kidney 293 T (HEK 293 T) cells. Stable transfectants were identified by both quantitative-PCR and immunoblotting.

2.8. Immunofluorescence staining and confocal microscopy

Cells were washed and fixed with 4% paraformaldehyde in PBS for 25 min, permeabilized with PBS/0.1% Triton X-100 for 5 min, and blocked with 3% BSA in PBS for 1 h. The permeabilized cells were then incubated overnight at 4 °C with the primary antibody against CD146 (1:100) and with Alexa Fluor 488 Phalloidin (1:2000) in PBS containing 3% BSA. Cells were washed three times with PBS/0.1% Tween 20, and then incubated for 1 h with a fluorescence-conjugated secondary antibody at a dilution of 1:300 at 37 °C. After 45 min, the cells were washed with PBS/0.1% Tween 20, and counterstained with 4′,6-diamidino-2-phenylindole (DAPI) to detect DNA. A confocal laser scanning microscope (Olympus FLUOVIEW FV1000, Tokyo, Japan) mounted with an Olympus IX81 digital camera was used for image acquisition.

2.9. Migration assay

Cell migration was analyzed using a Boyden chamber assay. Cells (1×10^5) were resuspended in DMEM and added to the upper chambers of 24-well Transwell plates (Costar, 8-μm pore size; Corning, USA). Complete medium (200 μL) was then added to the lower chamber as an attractant. After incubation for 7 h at 37 °C, cells remaining on the upper surface of the membrane were removed by swabbing with Q-tips. Cells that had migrated to the lower membrane surface are representative of migratory cells. After fixation with 20% methanol the cells were stained with crystal violet for visualization. These cells were counted at 20 × magnification and plotted as the number of migratory cells.

2.10. Wound healing assay

Cell monolayers, grown to confluence in a 6-well plate, were scratched using a 200 μl sterile pipette tip. Images of wounded monolayers were photographed under an inverted microscope at the time of wounding (0 h), at 6 h, and at 18 h.

2.11. Clinical sample collection

Ovarian cancer tissue specimens were obtained from patients at the Beijing Anzhen Hospital. Written informed consent was obtained from each patient, and prior to sample collection, ethical approval was obtained from the Ethics Committee of Anzhen Hospital and the Institute of Biophysics, Chinese Academy of Sciences. Samples were fixed in neutral buffered formalin, and then embedded in paraffin for immunohistochemistry. Detailed clinico-pathological information of these patient cohorts is provided in Tables S1–S2.

2.12. Immunohistochemistry

For DAB staining, a commercial human tissue array was deparaffinized and stained for both CD146 (1:100) and E-cadherin (1:100), and then incubated with a biotin-conjugated anti-mouse secondary antibody (ZSGB-BIO, Beijing, China) and horseradish peroxidase-conjugated streptavidin (Thermo Fisher, Waltham, USA). Binding was detected using a DAB solution (ZSGB-BIO). The tissues were then counterstained using hematoxylin (ZSGB-BIO). Images of the stained tissue samples were obtained using an OLYMPUS BX51 microscope equipped with an UPlan FL N digital camera (Tokyo, Japan).

2.13. Luciferase reporter assay

Cells (1×10^4) were transfected with 0.2 μg of a reporter construct and 4 ng of pRL-TK (Promega, Madison, USA) using Lipofectamine™ 2000 reagent (Invitrogen, Carlsbad, USA). After 24 hof transfection, the cells were treated with or without TGF-β1as indicated in the respective figures. Both firefly and *Renilla*luciferase activities were measured using a dual luciferase reporter assay system in a Glomax multi-detection system luminometer (Promega, Madison, USA). Firefly luciferase activity was normalized against *Renilla*luciferase activity, which was detected by co-transfection with pRL-TK in all reporter experiments. Luciferase activity in transfected cells was normalized against that of cells transfected with the pGL3-E control vector. Relative luciferase activities were expressed as fold increase over the paired control cells. The pGL3-E-Twist-wild type (WT) plasmid was constructed by PCR amplification and insertion of the mouse Twist promoter region (approximately −500 base pair from ATG). The primers used for PCR amplification were as follows: forward, 5′-TCC CCC ACC TTA AAT GTA TG-3′; reverse, 5′-GCG CCC CGT TCC GGC CTGG-3′. The plasmids pGL3-E-Twist-mutant-1 (MT-1), mutant-2 (MT-2), and mutant-2 (MT-3) were constructed by deletion of the STAT3 transcription factor binding site 1, binding site 2, and binding sites 1/2, respectively.

2.14. Statistical analysis

Statistical tests used to analyze data included the Fisher's exact

test,Log-rank test, Chi-square (χ^2) test, and Student's *t*-test. Multivariate statistical analysis was performed using a Cox regression model. Statistical analysis was performed using SPSS for Windows (16.0; SPSS, Inc. Armonk, USA) and GraphPad Prism (Prism 5.0; GraphPad Software Inc., La Jolla, USA) packages. A p value < 0.05 was considered statistically significant.

3. Results

3.1. CD146 expression is responsive to TGF-β signaling

Although CD146 is an inducible protein, and is upregulated in diverse malignant cancers [34–36], the tumor micro-environmental factors that can induce its expression are unclear. Our previous reports have shown that CD146 is functionally related and exhibits functions similar to an array of well-known EMT inducers including fibroblast growth factor (FGF) [38], vascular endothelial growth factor (VEGF)-A [39], platelet-derived growth factor (PDGF) [40], and Wnt [41]. We therefore selected these, along with other significant inducers of EMT, namely TGF-β1 and BMP, to simulate tumor microenvironmental signals. Among these factors, TGF-β1, BMP, and VEGF-A were found to induce CD146 upregulation in MEFs. In these MEFs, CD146 induction by VEGF-A was modest, whereas there was a robust increase in CD146 expression in response to BMP4 and TGF-β1 (Fig. 1A).

In vertebrates, the downstream intracellular effectors of TGF-β signaling include eight SMADs, i.e., SMAD1 to SMAD8. Among these, SMAD4 is a common SMAD, whereas SMAD6 and SMAD7 are inhibitory SMADs; and the remaining members are receptor-activated SMADs (R-SMADs). R-SMADs 2 and 3 are activated by TGF-β ligands, whereas R-SMADs 1, 5, and 8 are activated by BMP [42,43]. To assess the requirement for CD146 in TGF-β-induced EMT, we specifically knocked out CD146 in MEFs using the CRISPR/Cas9 technology, and established a CD146 knockout ($CD146^{KO}$) MEF cell line (Fig. 1B, Fig. S1). The lack of CD146 expression in $CD146^{KO}$ MEFs was confirmed by immunoblotting (Fig. S2).

Following this, we examined the induction of CD146 in response to different doses of TGF-β or BMP. In $CD146^{WT}$ MEFs, 3 ng/mL TGF-β or BMP induced a robust increase in CD146 expression (approximately 10 fold), but no dose response was observed (Fig. 1C and D). We also noted that there were no significant differences in the activation of SMAD2/3 by TGF-β1 or the activation of SMAD1/5 by BMP4, between $CD146^{WT}$ MEFs and $CD146^{KO}$ MEFs. The phosphorylation levels of R-SMADs were also not affected by CD146 induction (Fig. 1C and D). These data indicate that CD146 is an inducible protein responsive to TGF-β signaling, and further suggest that CD146 upregulation in cancers may be caused by TGF-β presence in the tumor microenvironment.

3.2. CD146 induction by TGF-β does not affect the expression of SMADs

To further explore CD146 upregulation by TGF-β signaling, the time-course of CD146 induction in response to TGF-β1 or BMP4 was analyzed. In both cases, CD146 was upregulated in $CD146^{WT}$ MEFs in a time-dependent manner (Fig. 2A and B).

Consistent with the lack of difference in TGF-β1-induced R-SMAD activation between $CD146^{WT}$ and $CD146^{KO}$ MEFs shown in Fig. 1, there were no differences observed in the time course of R-SMADs activation by TGF-β1 between these two cell lines. In addition, there were no differences in the expression levels of SMAD1, 2, 3, 5, or 8 betweenCD146^{WT} and $CD146^{KO}$ MEFs (Fig. 2C and D).

SMAD4 is a common SMAD that facilitates translocation of R-SMADs into the nucleus to initiate transcription of hundreds of genes [43,44]. We examined the expression of SMAD4 inCD146^{WT} and $CD146^{KO}$ cells in the presence or absence of TGF-β or BMP stimulation. The data showed that there were no differences in the expression of SMAD4 between the two cell lines; furthermore, stimulation with TGF-β or BMP did not affect SMAD4 levels in either of these two cell lines (Fig. 2E and F).

SMAD6 and SMAD7 are known to be highly regulated by extracellular signals. They act as respective 'inhibitory' SMADs for BMP and TGF-β signaling branches [43]. Consistent with the lack of difference in phospho-SMAD2/3 and phospho-SMAD1/5 levels between $CD146^{WT}$ and $CD146^{KO}$ cells, there was no obvious expression change in SMAD6 or SMAD7 between these two different cell lines. In addition, treatment with BMP and TGF-β did not affect the levels of SMAD6 or SMAD7 in these two cell lines (Fig. 2E and F). These data indicate that CD146 is not involved in the SMAD-dependent canonical TGF-β signaling pathway.

3.3. CD146 mediates an E-cadherin to N-cadherin switch following TGF-β signaling

Based on our previous report that the overexpression of exogenous CD146 in $CD146^{-}$ MCF7 cells can induce EMT [45], and the fact that TGF-β is a potent EMT inducer that controls the E-to N-cadherin switch [20,21,28], we next investigated the role of CD146 in TGF-β-induced EMT. To induce a transient EMT, $CD146^{WT}$ or $CD146^{KO}$ MEFs were treated with 10 ng/mL of TGF-β1 or BMP4 for 12 h and 24 h. SMAD2/3 and SMAD1/5 were activated in response to TGF-β1 and BMP4 as expected (Fig. 3A). Interestingly, compared with $CD146^{WT}$ cells, CD146 deficiency led to inversion of the E-cadherin and N-cadherin expression patterns. In $CD146^{KO}$ cells, E-cadherin expression was upregulated in the absence of TGF-β1 or BMP4 compared to $CD146^{WT}$ cells, and was further induced following TGF-β1 or BMP4 treatment. In contrast, $CD146^{KO}$ cells showed reduced N-cadherin expression compared to that in $CD146^{WT}$ cells, and a lack of N-cadherin induction following treatment with TGF-β1 or BMP4 (Fig. 3A).

To further confirm that CD146 is necessary and sufficient for the E-to N-cadherin switch, we reconstituted CD146 expression in $CD146^{KO}$ cells by transfecting GFP-tagged CD146 into this cell line. The expression of GFP or RFP did not change the expression patterns in $CD146^{WT}$ or $CD146^{KO}$ MEFs. The E-cadherin and N-cadherin expression levels in $CD146^{KO}$ cells with CD146 overexpression were restored to those in $CD146^{WT}$ cells (Fig. 3B), *i.e.*, the E-cadherin levels were reduced and in parallel, the N-cadherin levels were increased. Taken together, these data suggest that CD146 is required for the TGF-β-induced E-to N-cadherin switch.

Next, we observed the effect of CD146 knockout on the morphology of $CD146^{KO}$ MEFs. Compared to $CD146^{WT}$ MEFs, loss of CD146 triggered a change in cell morphology from an elongated shape to a cobble stone-like morphology, and also caused a decrease in the number of fibroblast-like stress fibers (Fig. 3C). In addition, the $CD146^{KO}$ MEFs showed reduction in the morphological changes when the cells were treated with TGF-β (Fig. S3). This association of CD146 with cytoskeletal remodeling suggests that CD146 induces EMT.

Therefore, we further examined the correlation between CD146expression levels and the E-to N-cadherin switch by CD146 overexpression ($CD146^{OE}$) in $CD146^{WT}$ MEFs. Elevated levels of CD146 in $CD146^{OE}$ MEFs compared with those in $CD146^{WT}$ MEFs were confirmed by western blotting. Next, the expression of E-cadherin and N-cadherin in $CD146^{OE}$, $CD146^{WT}$, and $CD146^{KO}$ MEFs was examined. There was a negative correlation between CD146 levels and E-cadherin levels, and a positive correlation between CD146 levels and N-cadherin levels in these three cell lines that expressed different levels of CD146 (Fig. 3D). A transwell assay revealed that increased cell motility showed a significant positive correlation with CD146 expression levels (Fig. 3E and F). In summary, these data show that CD146 is required for the TGF-β-induced switch from E-cadherin to N-cadherin, suggesting that CD146 may play a critical role in the EMT process.

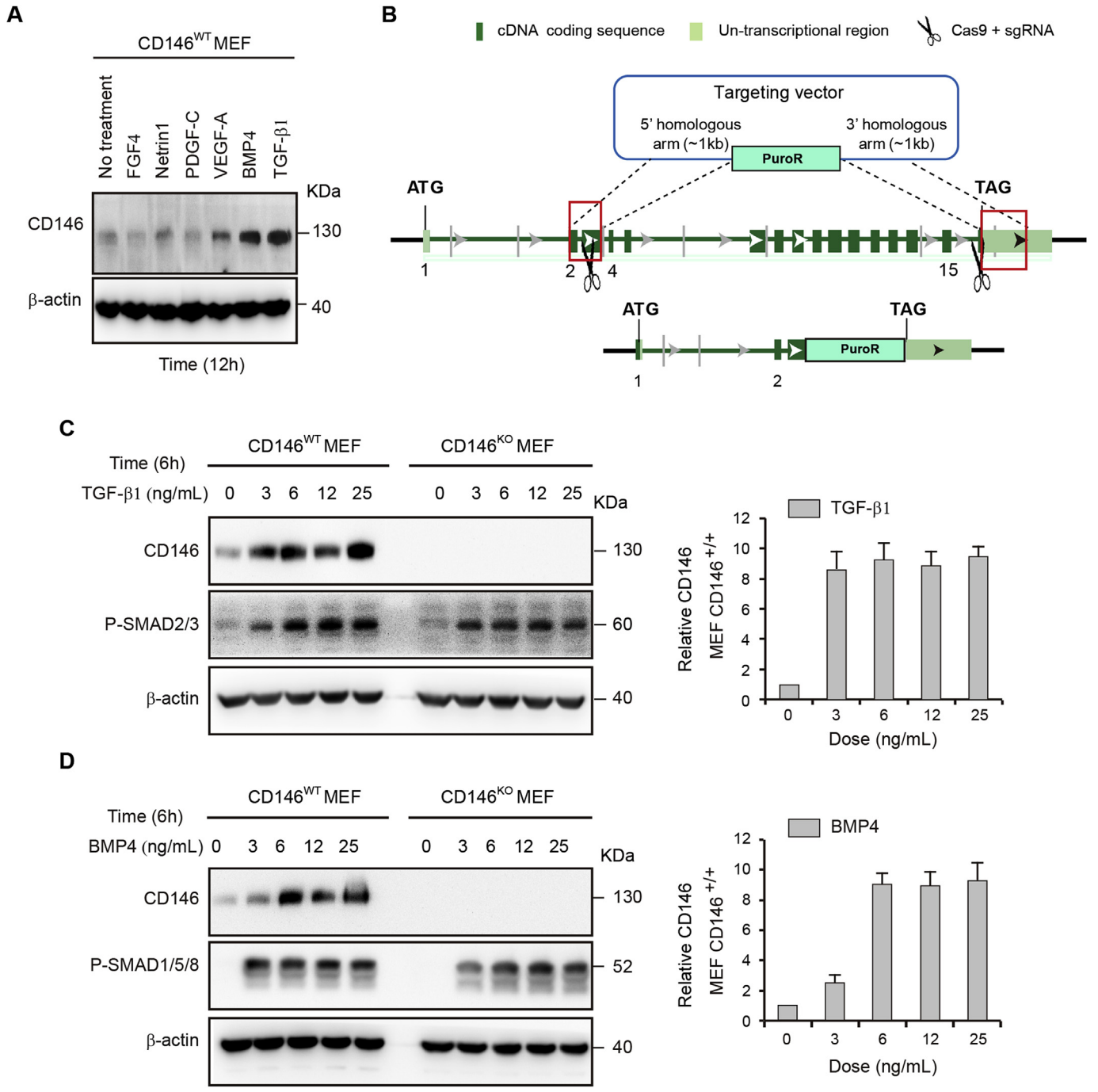

Fig. 1. Induction of CD146 expression upon stimulation of TGF signaling. (A) Induction of CD146 expression after treatment of MEFs with the indicated EMT-inducing factors (FGF4, 10 ng/mL; Netrin-1, 250 ng/mL; PDGF-C, 100 ng/mL; VEGF-A, 10 ng/mL; BMP2, 25 ng/mL; and TGF-β1, 10 ng/mL) was examined by immunoblotting using an anti-CD146 antibody. Equal protein loading was estimated by assessing the levels of β-actin expression under each condition. (B) Schematic of the mouse *cd146* gene showing the CRISPR/Cas9-target sites. Individual exons are shown as boxes. The arrow indicates the direction of transcription. Exons 3–16 were replaced with a puromycin (Puro) resistance cassette. (C and D) CD146 protein expression in wild-type ($CD146^{WT}$) and CD146 knockout ($CD146^{KO}$) MEFs after 6 h stimulation with different doses of TGF-β1 (3–25 ng/mL, in C) or BMP4 (3–25 ng/mL, in D) was examined by immunoblotting. The band densities (mean ± s.e.m.) for CD146 were measured in at least three independent immunoblots, and were normalized to those of β-actin (loading control). The signal from untreated cells was set as one.

3.4. CD146 induces the E-cadherin to N-cadherin switch in human ovarian cancer cells

Our previous study has shown that CD146 expression is positively and significantly correlated with malignancy in cervical and endometrial cancers [33]. We wondered whether such a correlation also existed in another type of gynecological cancer, *i.e.,* ovarian cancer, and whether CD146 could induce EMT in ovarian cancer cells. To investigate CD146 expression in ovarian cancer, we conducted an immunohistochemical study using the AA1 anti-CD146 antibody on samples collected from 124 normal and cancerous tissues. As summarized in Tables S1 and S2, CD146 was detected in a large number of ovarian cancer samples, especially in those with FIGO Stages III-IV, suggesting that CD146 is positively associated with the malignant

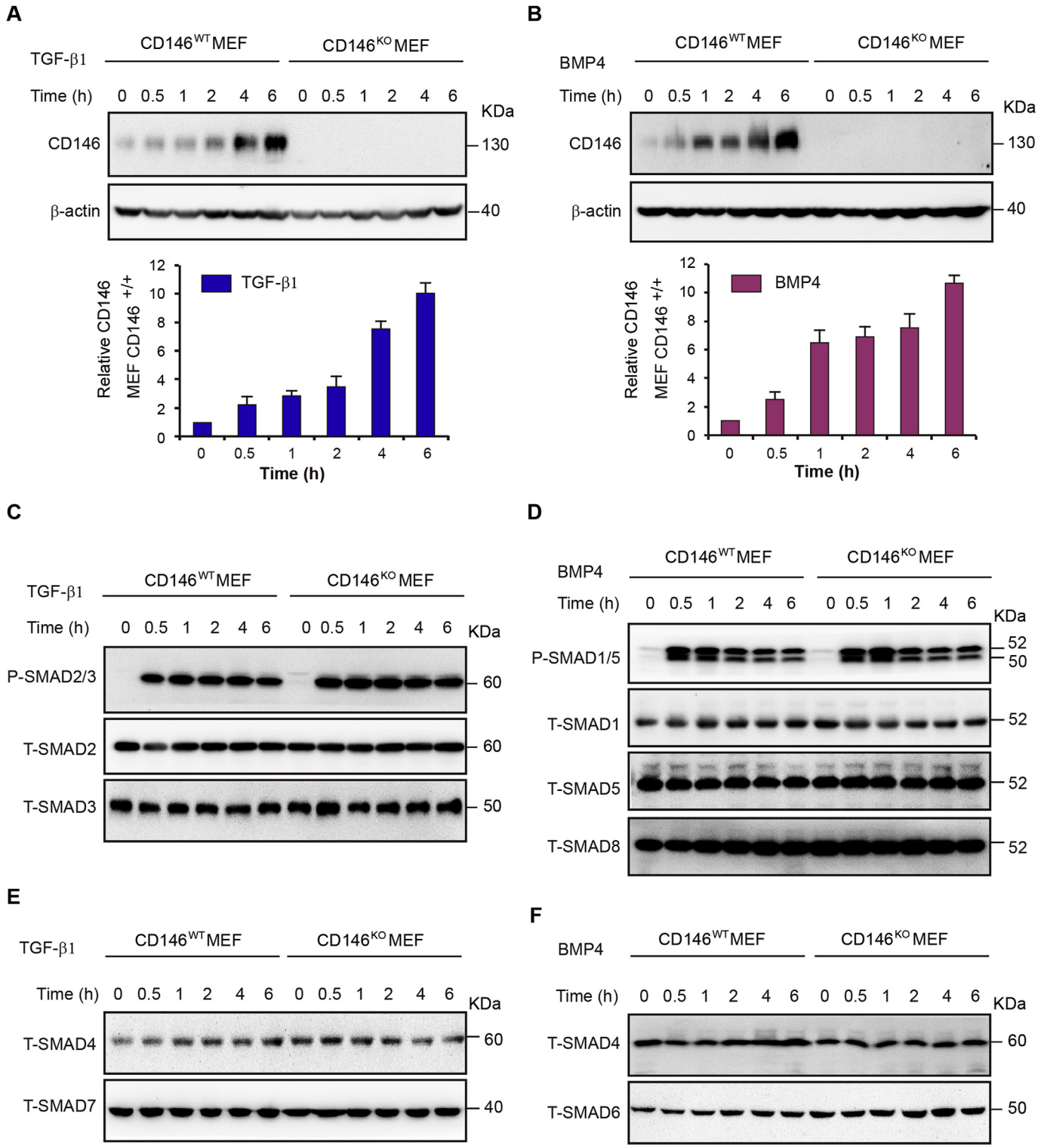

Fig. 2. Time-dependent induction of CD146 by TGF signaling. (A and B) Expression of CD146 in CD146^{WT}or CD146^{KO} MEFs was examined by immunoblotting after stimulation with TGF-β1 (10 ng/mL, in A) or BMP4 (10 ng/mL, in B) for the indicated times. Band densities (mean ± s.e.m.) for CD146 were measured in at least three independent immunoblots and normalized to those of β-actin (loading control). The signal from untreated cells was set as one. (C and D) CD146^{WT}or CD146^{KO} MEFs were stimulated with either TGF-β1 (10 ng/mL, in C) or BMP4 (10 ng/mL, in D) for the indicated times, and the expression and activation levels of SMAD2 and SMAD3 (C) or SMAD1 and SMAD5, as well as the expression of SMAD8 (D) were examined by immunoblotting. (E and F) CD146^{WT}or CD146^{KO} MEFs were stimulated with either TGF-β1 (10 ng/mL, in E) or BMP4 (10 ng/mL in F) for the indicated times and the expression levels of SMAD4 and SMAD7 in E or SMAD4 and SMAD6 in F were assessed by immunoblotting.

phenotype in ovarian cancers, further strengthening the connection between CD146 and EMT and metastasis.

We then selected the CD146^{+} SKOV3 ovarian cancer cell line to examine the CD146 response to TGF-β signaling. As shown in Fig. 4A and B, CD146 was up-regulated in SKOV3 cells following stimulation with TGF-β1 or BMP4. These data suggest that TGF-β- mediated

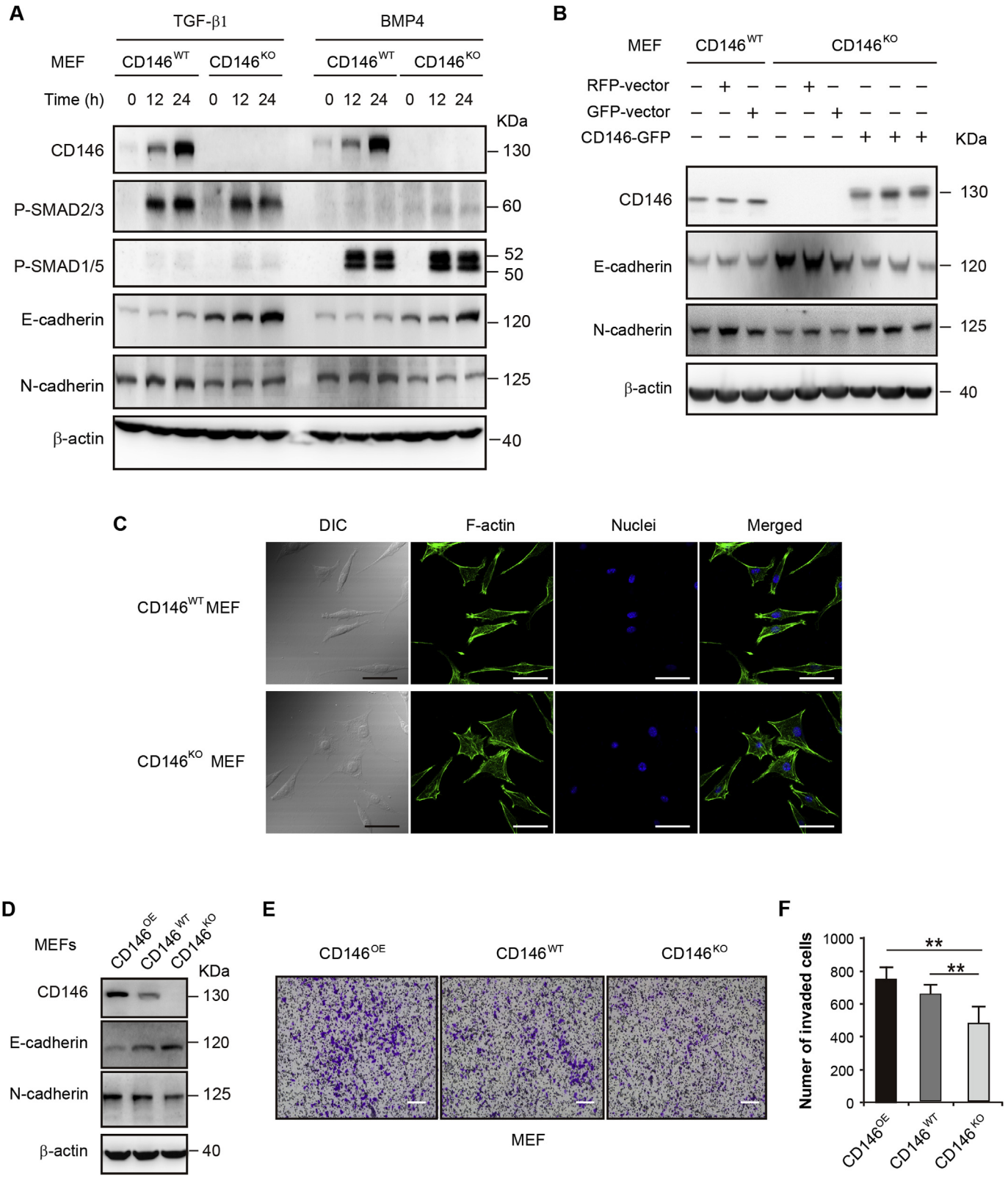

Fig. 3. CD146 mediates the E-cadherin-to-N-cadherin switch during TGF-β signaling-induced EMT in MEFs. (A) Expression levels of CD146 and the EMT markers, E-cadherin and N-cadherin, were analyzed by immunoblotting following treatment of $CD146^{WT}$ or $CD146^{KO}$ MEFs with 10 ng/mL TGF-β1 or BMP4 for the indicated times. Activation of SMAD2/3 by TGF-β1 and SMAD1/5 by BMP2 was also examined. (B) Immunoblotting analysis of CD146, E-cadherin, and N-cadherin in $CD146^{WT}$, $CD146^{KO}$, or $CD146^{KO}$ MEFs transfected with pEGFP-N1, pRGFP-N1, or pEGFP-N1-CD146. (C) Immunofluorescence images of the F-actin cytoskeletal organization in $CD146^{WT}$ (upper panel) and $CD146^{KO}$ (lower panel) MEFs. Nuclei are stained with DAPI (blue). Scale bar = 50 μm. (D) Immunoblotting analysis showing the correlation between CD146 expression and the expression of E-cadherin and N-cadherin in CD146overexpressing ($CD146^{OE}$), $CD146^{WT}$, and $CD146^{KO}$ MEFs. (E and F) Migration assays using $CD146^{OE}$, $CD146^{WT}$, and $CD146^{KO}$MEFs. Representative images of the migrated or invaded cells are shown in E. Scale bar = 200 μm.Data were collected from three independent experiments, $^{**}P < 0.01$, compared with $CD146^{KO}$MEFs in F. (For interpretation of the references to colour in this figure legend, the reader is referred to the Web version of this article.)

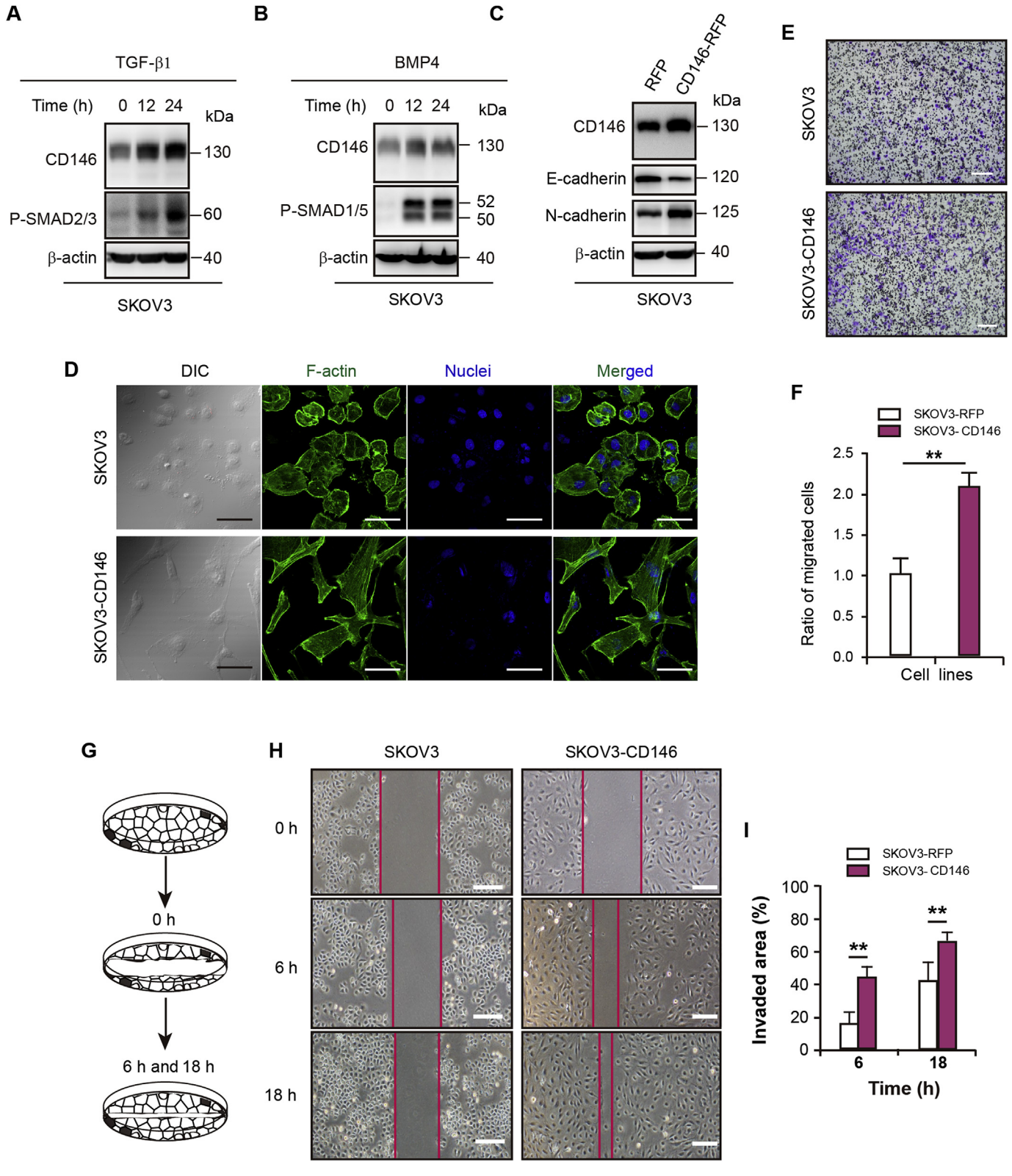

(caption on next page)

induction of CD146 expression might be a common feature in mammalian cells.

To simulate CD146 induction by TGF-β signaling, SKOV3 cells were transfected with the pERFP-N1-CD146 vector (Fig. 4C), which encodes CD146 tagged at its amino terminus with RFP. Compared to SKOV3 cells transfected with RFP alone, E-cadherin expression levels were reduced and those of N-cadherin were significantly increased along with the expected increase in CD146 expression in SKOV3-CD146-RFP cells, demonstrating that CD146 also mediates the E-to N-cadherin switch in ovarian cancer cells.

Furthermore, SKOV3-CD146-RFP cells had a dramatically different morphology compared with the wild-type SKOV-RFP cells. CD146

Fig. 4. CD146 induces EMT in human ovarian cancer cells. (A and B) Induction of CD146 expression following 10 ng/mL TGF-β1 or BMP4 treatment in SKOV3 cells was assessed by immunoblotting. Activation of SMAD2/3 by TGF-β1 and SMAD1/5 by BMP4was also examined. (C) Immunoblotting analysis showing the correlation between CD146 expression levels and E-cadherin and N-cadherin expression levels in SKOV3 cells. Cells were transfected with empty vector pERFP-N1 or pERFP-N1-CD146. (D) Immunofluorescence images of the F-actin cytoskeletal organization in SKOV3-RFP cells (upper panel) and SKOV3 cells overexpressing CD146 (SKOV3-CD146, lower panel). Nuclei are stained with DAPI (blue). Scale bar = 50 μm. (E and F) Migration assay using SKOV3-RFP and SKOV3-CD146 cells. Representative images of migrated or invaded cells are shown in E. Scale bar = 200 μm. Quantification of cell migration or invasion data, collected from three independent experiments, $^{**}P < 0.01$, compared with SKOV3 cells in F. (G) Schematic of the overall procedure used to assess wound healing. (H) Phase contrast photographs of SKOV3-RFP (left) and SKOV3-CD146 (right) cells taken at 0 h (immediately after scratching), and at the indicated times showing wound closure. Scale bar = 200 μm. (I) Quantification of cell invasion into the wounded area at different time points in SKOV3-RFP and SKOV3-CD146 cells represented as percentage of the wounded area at time 0. Results represent the mean of three measures for each wounded area, and were obtained using duplicate biological samples. Error bars indicate SEM (n = 8). $^{**}P < 0.01$, compared with SKOV cells. (For interpretation of the references to colour in this figure legend, the reader is referred to the Web version of this article.)

overexpression in SKOV3 cells triggered the transition from a cobble stone-like morphology to an elongated shape associated with increased cell scattering. In addition, the number of fibroblast-like stress fibers were increased (Fig. 4D). Both a transwell assay and a wound healing assay showed that there was an increase in cell motility that was positively and significantly correlated with CD146 protein levels (Fig. 4E and I). In summary, these data clearly show that CD146 is required for the TGF-β-induced cadherin switch and EMT in ovarian cancer cells.

3.5. CD146 expression is positively associated with a higher metastatic potential

In ovarian cancers, CD146 expression was enhanced in the clinical samples of cancerous gynecological tissues compared with their normal counterparts (Fig. 5A). Fluorescent immunohistochemistical assays showed that CD146 was detected mainly in the membranes and cytoplasm (Fig. 5B). The 106 patients representing all four stages of ovarian cancer were divided in two groups based on the presence or absence of CD146 by immunohistochemistry (IHC). Kaplan–Meier survival curves showed that CD146 expression was clearly correlated with patient survival rate. The $CD146^+$ group was associated with a statistically significant ($P = 0.017$) decrease in overall survival time, with a 2.3-fold higher risk of death (Fig. 5C).

Loss of E-cadherin has frequently been associated with poor prognosis and survival in patients with various cancers [46]. Thus, we next asked if the negative prognostic correlation corresponded with the loss of E-cadherin in the $CD146^+$ group. To perform this analysis, we analyzed 29 tissue samples taken from human ovarian cancers with a histological grade of 3. Among these samples, only six of 29 specimens were $CD146^-$ and E-$cadherin^-$. The remaining 23 $CD146^+$ specimens were E-$cadherin^-$ (Fig. 5D and E and S4). These results further strengthened the connection between CD146 and EMT and metastasis.

3.6. CD146 is associated with ERK- and STAT3-activation and twist upregulation

TGF-β triggers canonical SMAD-dependent signaling as well as non-canonical SMAD-independent pathways, such as those involving mitogen activated protein kinases (MAPKs) [47–50]. To explore how CD146 regulates the E-to N-cadherin switch, the major non-canonical pathways were examined in $CD146^{WT}$ and $CD146^{KO}$ MEFs following treatment with either TGF-β1 or BMP4. We first investigated whether activation of different MAPKs was affected by TGF-β-induced CD146 expression by measuring the phosphorylation (reflective of activation) of ERK, p38, and JNK in $CD146^{WT}$ and $CD146^{KO}$ MEFs with or without TGF-β1 or BMP4 stimulation. As shown in Fig. 6A, following either TGF-β1 or BMP4 stimulation, the levels ofp38 and JNK phosphorylation were similar between $CD146^{WT}$ and $CD146^{KO}$ MEFs, and did not appear to be activated by either TGF-β1 or BMP4. In contrast, the basal levels of ERK phosphorylation were higher in $CD146^{WT}$ MEFs compared to $CD146^{KO}$ MEFs, and were increased by either TGF-β1 or BMP4 treatment at the time points examined. Thus, deficiency of CD146 appears specifically to contribute to decreased ERK activation in $CD146^{KO}$ cells. Therefore, it is possible that CD146 contributes to the E-to N-cadherin switch through ERK activation.

Because both CD146 and TGF-β signaling are implicated in immunity [34,43], we examined whether activation of NF-κB and STAT3, two key transcriptional factors important in the immune response, was affected by CD146 induction. As shown in Fig. 6B, the phosphorylation levels of p65, a subunit of NF-κB, were comparable in $CD146^{WT}$ and $CD146^{KO}$ MEFs both before and after stimulation with TGF-β1 or BMP4. In contrast, STAT3 phosphorylation was significantly increased by TGF-β1 or BMP4 treatment of $CD146^{WT}$ MEFs and was sustained up to 24 h post-stimulation. In contrast, there was modest increase in STAT3 phosphorylation following stimulation with TGF-β1 or BMP4 in $CD146^{KO}$ MEFs. Thus, CD146 specifically appears to contribute to the prolonged activation of STAT3.

EMT-TFs are engaged in the suppression of E-cadherin expression in various EMT processes and malignancies [51]. Because E-cadherin expression was increased in $CD146^{KO}$ MEFs, we wondered which EMT-TFs are affected by CD146 and contribute to such a change. Immunoblotting showed that the expression of Twist, but not Snail1, Snail2 (Slug), or Zeb1, was positively correlated with CD146 expression (Fig. 6C). This correlation was further confirmed in the three MEF cell lines with different levels of CD146 expression, namely $CD146^{OE}$, $CD146^{WT}$, and $CD146^{KO}$ MEFs (Fig. 6D).

To further confirm the requirement for CD146 in sustaining STAT3 activation and in upregulating the expression levels of Twist, GFP-tagged CD146 was overexpressed in $CD146^{KO}$ MEFs to reconstitute CD146 expression. The data showed a positive association between CD146 expression and TGF-β1-induced activation of STAT3 and ERK, and restoration of Twist upregulation (Fig. 6E), indicating that CD146 presence and its induction are required for STAT3 activation and Twist upregulation.

3.7. CD146 mediates the E-cadherin to N-cadherin switch through STAT3/Twist and ERK pathways

Although STAT3 is reported as a potent EMT inducer that inhibits E-cadherin expression, the EMT-TF that is the transcriptional target of STAT3 remains controversial [52]. We therefore analyzed the core promoter regions of four EMT-TFs, encompassing a 2000 base pair sequence upstream of the transcriptional start site (+1) in each gene. Bioinformatics analysis using the TFSEARCH program (version 1.3) revealed that only the mouse Twist promoter region contained two consensus binding sites for STAT3, *i.e.*, A (−117/-109) and B (−131/-121). We thus generated four constructs of the mouse Twist promoter linked to a luciferase reporter, namely the wild type (pGL3-E-Twist-WT) reporter and three mutant reporters with the STAT3-binding sites specifically deleted, *i.e.*, deletion of the A site (pGL3-E-Twist-ΔSTAT3-A), the B site (pGL3-E-Twist-ΔSTAT3-A), and both A/B sites together (pGL3-E-Twist-ΔSTAT3-A/B) (Fig. 7A).

Next, we examined whether TGF-β induces Twist expression through trans-activation of the Twist gene promoter. Strikingly, TGF-β1 significantly activated the WT Twist promoter with an induction level similar to that seen for Twist protein in $CD146^{WT}$ and $CD146^{KO}$ cells.

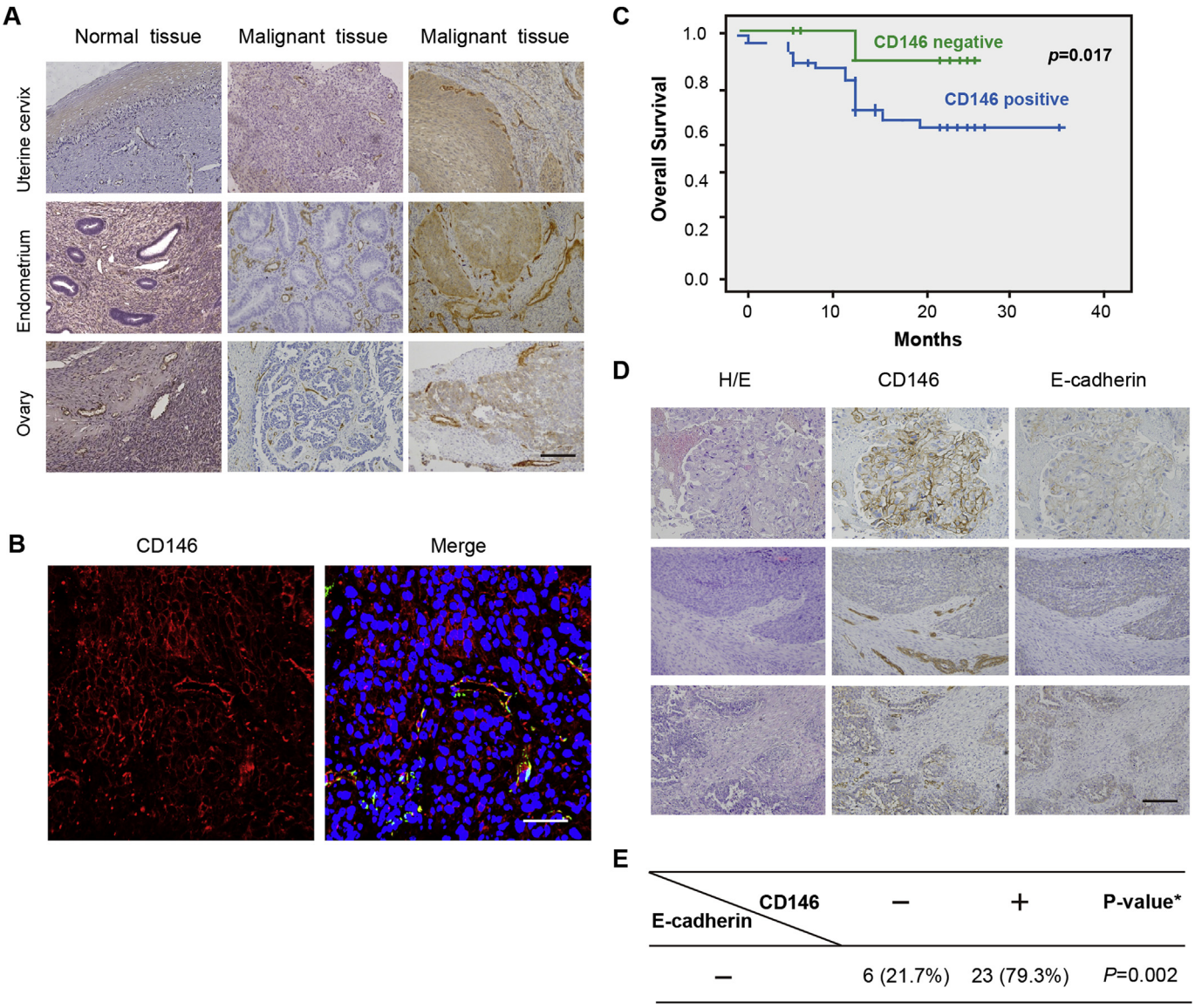

Fig. 5. CD146 is associated with ovarian cancer. (A) Expression of CD146 in the clinical samples of normal and cancerous gynecological tissues. Representative immunohistochemical staining of CD146 in the clinical samples. (B) Immunofluorescence images of CD146 in ovarian cancer samples. Nuclei are stained with DAPI (blue). (C) Kaplan–Meier progression-free survival curves showing the difference between CD146-and CD146^{+} groups. (D) Representative immunohistochemical staining of CD146 and E-cadherin in samples of epithelial ovarian cancer. (E) Statistical correlation between CD146 expression and E-cadherin expression in epithelial ovarian cancers. A Pearson's χ^2 test was used to determine the correlation. $P < 0.05$ was considered significant. Scale bar = 200 μm. (For interpretation of the references to colour in this figure legend, the reader is referred to the Web version of this article.)

However, in these cell lines, Twist promoter activity was significantly reduced in the absence of the STAT3-binding site A, B, or A/B (Fig. 7B), indicating that STAT3 is required for the TGF-β-induced upregulation of Twist.

E-cadherin expression is negatively correlated with STAT3 and Twist. To examine whether STAT3/Twist is involved in the CD146-mediated E-to N-cadherin switch, we treated CD146^{WT} and CD146^{KO} cells with the selective STAT3 inhibitor NSC74859, either alone or in combination with TGF-β1. As a result, the STAT3 inhibitor dramatically blocked the upregulation of STAT3 and Twist, and in addition, reversed the suppression of E-cadherin expression. In contrast, the STAT3 inhibitor had little effect on N-cadherin expression. These data indicate that the STAT3/Twist pathway is involved in CD146-mediated inhibition of E-cadherin expression (Fig. 7C).

ERK activation is reportedly associated with the upregulation of N-cadherin [53] and downregulation of E-cadherin [54]. We found that the ERK inhibitor U0126 blocked N-cadherin expression, whereas it had little effect on E-cadherin expression. Taken together, these data indicate that the ERK pathway is involved in the upregulation of N-cadherin in MEFs (Fig. 7D). Furthermore, these data also indicate that CD146 sufficiency is required for the TGF-β1-induced inhibition of E-cadherin expression and N-cadherin upregulation.

4. Discussion

A thorough understanding of the EMT process will facilitate a better understanding of cancer metastasis, which is the major barrier to cancer patient survival. Here, we reveal how CD146 mediates the E-cadherin to N-cadherin switch during TGF-β-induced EMT. This study suggests that a functional reversion of this cadherin switch may reduce the effects of TGF-β on the induction of the EMT itself, on malignancy, as well as on cancer metastasis.

Although numerous studies have focused on the mechanism underlying TGF-β signaling in EMT, the precise contributions of TGF-β

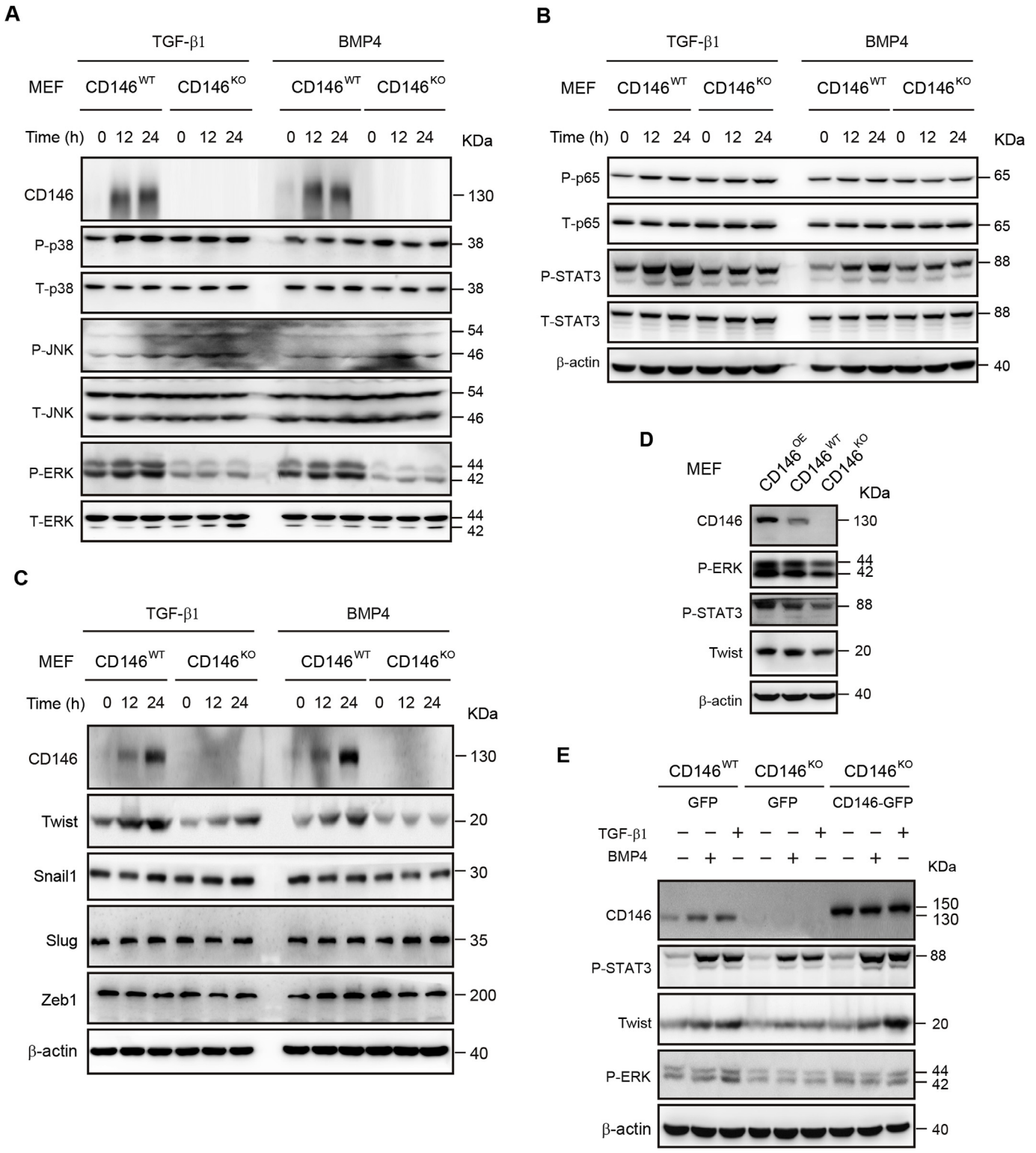

Fig. 6. CD146 is correlated with upregulation of ERK, STAT3, and Twist. (A–C) $CD146^{WT}$ and $CD146^{KO}$ MEFs were stimulated with either TGF-β1 (10 ng/mL) or BMP4 (10 ng/mL) for the indicated times. Expression of CD146 as well as the expression and activation of p38 MAPK, JNK, or ERK, was examined by immunoblotting in A. The expression and activation of p65 and STAT3 was examined by immunoblotting in B. The expression of the EMT-TFs Twist, Snail1, Slug (Snail2), and Zeb1 were examined by immunoblotting in C. (D) $CD146^{OE}$, $CD146^{WT}$, and$CD146^{KO}$ MEFswere immunoblotted to assess the basal levels of phospho-ERK, -STAT3, and Twist expression. (E) $CD146^{WT}$ transfected with pEGFP-N1, or $CD146^{KO}$ transfected with pEGFP-N1 or pEGFP-N1-CD146 were stimulated with either TGF-β1 (10 ng/mL) or BMP4 (10 ng/mL). The expression of CD146 and Twist, and the activation of STAT3 and ERK was assessed by immunoblotting.

signaling in EMT have not been fully clarified [28]. Our results showing cooperation between CD146 and TGF-β in EMT suggest that CD146-controlled signaling is a critical non-canonical pathway in TGF-β signaling. For this reason, simultaneously targeting of both CD146 and TGF-β signaling could have better efficacy with respect to cancer therapy compared to targeting either pathway alone.

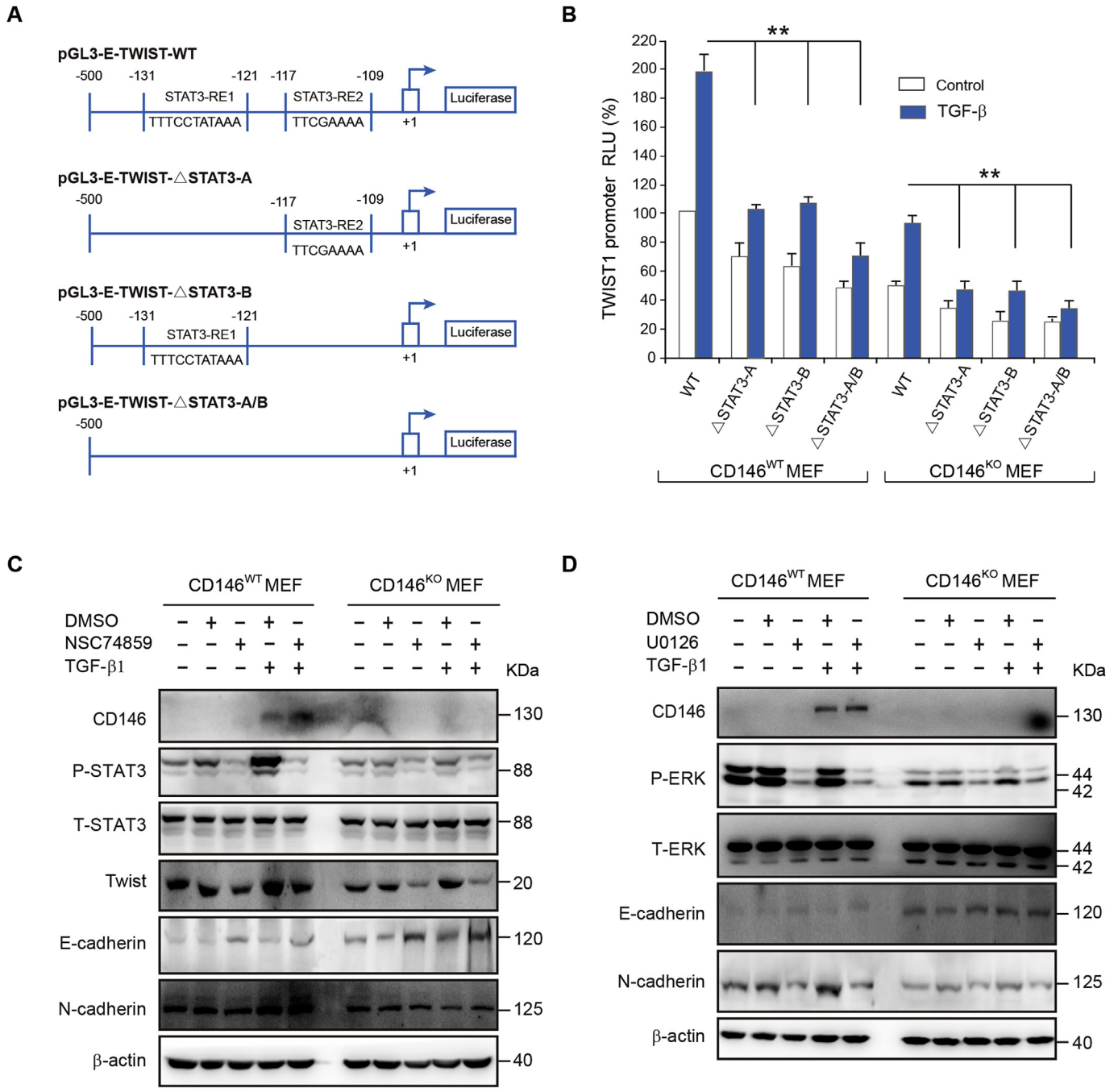

Fig. 7. CD146 mediates the E-cadherintoN-cadherin switch in TGF-β-induced EMT. (A) Diagrammatic representation of the mouse Twist luciferase reporters. The wild-type reporter of pGL3-E-Twist-WT is shown in the upper panel. Mutants with deletions of one of each or both STAT3-binding sites (pGL3-E-Twist-ΔSTAT3-A, pGL3-E-Twist-ΔSTAT3-Bor pGL3-E-Twist-ΔSTAT3-A/B) are shown in the lower panels. (B) $CD146^{WT}$ or $CD146^{KO}$MEFs were transfected with pGL3-E-Twist-WT, pGL3-E-Twist-ΔSTAT3-A, pGL3-E-Twist-ΔSTAT3-B, or pGL3-E-Twist-ΔSTAT3-A/B together with pRL-TK and stimulated with 10 ng/mL of TGF-β1. Luciferase activity was determined at 24 h after treatment. (C) Inhibition of STAT3 relieved the suppression of E-cadherin expression. $CD146^{WT}$ or $CD146^{KO}$ MEFs were stimulated with or without TGF-β1 (10 ng/mL) for 24 h in the presence or absence of the STAT3 inhibitor NSC74859 (200 μM). The expression of CD146, the expression and activation of STAT3, and the expression levels of E-cadherin, N-cadherin, and Twist were assessed by immunoblotting. (D) Inhibition of ERK suppresses N-cadherin expression. $CD146^{WT}$ or $CD146^{KO}$ MEFs were stimulated with or without TGF-β1 (10 ng/mL) for 24 h in the presence or absence of the ERK inhibitor U0126 (2 μM). The expression and activation of ERK and the expression of E-cadherin and N-cadherin was assessed by immunoblotting.

Accumulating evidence has shown that upregulation of N-cadherin is more important in cancer metastasis than the loss of E-cadherin [55,56]. Our previous study suggested that CD146-mediated inhibition of E-cadherin expression by enhancing Snail2 (Slug) expression might be a general feature common to all breast cancer cells [45]. Functional restoration of E-cadherin or depletion of N-cadherin has been show to inhibit tumor cell motility and invasion in some tumors [57,58]. Thus, our present findings that CD146 can simultaneously inhibit E-cadherin and upregulate N-cadherin strongly imply that CD146 is a crucial player in EMT progression.

EMT-TF-mediated suppression of E-cadherin expression is involved in various malignancies [28]. Our previous study revealed that in $CD146^{-}$ MCF-7 cells, forced overexpression of CD146 can upregulate Snail2 (Slug) expression [45]. The present study showed that CD146

expression is positively correlated with the expression of Twist, but not other EMT-TFs, reinforcing the notion that TGF-β can activate different EMT-TFs in different cellular contexts [28].

Our study implies that the CD146-STAT3-Twist axis represents a crucial cascade downstream of TGF-β signaling for inhibition of E-cadherin expression as well as EMT. STAT3 is known to be an essential non-canonical pathway in TGF-β-induced EMT [59–61]. In this regard, based on the fact that CD146 induction by TGF-β treatment occurred concurrently with the enhanced STAT3 activation and Twist upregulation, we speculate that the inhibition of E-cadherin expression by Twist relies at least partially on CD146-mediated STAT3 activation.

ERK signaling has been shown to modulate the expression of both E− and N-cadherin in a cell context dependent manner [53,62,63]. We found that the presence of CD146 is linked with sufficient ERK activation, as well as N-cadherin upregulation, suggesting that the CD146/ERK cascade is required for the increase in N-cadherin expression observed during the cadherin switch.

Taken together, our findings provide explicit evidence on how CD146 concurrently inhibits E-cadherin expression and upregulates N-cadherin expression in response to TGF-β, and will facilitate a better understanding of the key non-canonical pathways in TGF-β signaling involved in EMT as well as in cancer metastasis. Therefore, this study is expected to elucidate the general mechanism by which cells substitute E-cadherin with N-cadherin in order to initiate EMT and provides insights for targeting CD146 as an effective strategy in the treatment of cancer, especially in ovarian cancer.

Conflict of interest statement

The authors declare no competing financial interests.

Acknowledgements

This work was supported in part by grants from the National Natural Science Foundation of China (91529306), the Strategic Priority Program of the Chinese Academy of Sciences (XDA12020207) and the National Basic Research Program of China (#2015CB553705).

Appendix A. Supplementary data

Supplementary data related to this article can be found at http://dx.doi.org/10.1016/j.canlet.2018.05.016.

References

[1] C. Garbe, K. Peris, A. Hauschild, P. Saiag, M. Middleton, A. Spatz, J.J. Grob, J. Malvehy, J. Newton-Bishop, A. Stratigos, H. Pehamberger, A.M. Eggermont, F. European Dermatology, D.-O. European Association of, R. European Organization of, C. Treatment of, Diagnosis and treatment of melanoma. European consensus-based interdisciplinary guideline–Update 2012, Eur. J. Canc. 48 (2012) 2375–2390.
[2] J.M. Halbleib, W.J. Nelson, Cadherins in development: cell adhesion, sorting, and tissue morphogenesis, Genes Dev. 20 (2006) 3199–3214.
[3] I.R. Beavon, The E-cadherin-catenin complex in tumour metastasis: structure, function and regulation, Eur. J. Canc. 36 (2000) 1607–1620.
[4] A. Mariotti, A. Perotti, C. Sessa, C. Ruegg, N-cadherin as a therapeutic target in cancer, Expet Opin. Invest. Drugs 16 (2007) 451–465.
[5] R.B. Hazan, G.R. Phillips, R.F. Qiao, L. Norton, S.A. Aaronson, Exogenous expression of N-cadherin in breast cancer cells induces cell migration, invasion, and metastasis, J. Cell Biol. 148 (2000) 779–790.
[6] R.B. Hazan, R. Qiao, R. Keren, I. Badano, K. Suyama, Cadherin switch in tumor progression, Ann. N. Y. Acad. Sci. 1014 (2004) 155–163.
[7] G. Li, K. Satyamoorthy, M. Herlyn, N-cadherin-mediated intercellular interactions promote survival and migration of melanoma cells, Canc. Res. 61 (2001) 3819–3825.
[8] M.J. Wheelock, Y. Shintani, M. Maeda, Y. Fukumoto, K.R. Johnson, Cadherin switching, J. Cell Sci. 121 (2008) 727–735.
[9] M.A. Nieto, The ins and outs of the epithelial to mesenchymal transition in health and disease, Annu. Rev. Cell Dev. Biol. 27 (2011) 347–376.
[10] J.P. Thiery, H. Acloque, R.Y. Huang, M.A. Nieto, Epithelial-mesenchymal transitions in development and disease, Cell 139 (2009) 871–890.
[11] M. Guarino, Epithelial-mesenchymal transition and tumour invasion, Int. J. Biochem. Cell Biol. 39 (2007) 2153–2160.
[12] E.D. Hay, An overview of epithelio-mesenchymal transformation, Acta Anatomica 154 (1995) 8–20.
[13] J.P. Thiery, J.P. Sleeman, Complex networks orchestrate epithelial-mesenchymal transitions, Nature reviews, Mol. Cell Biol. 7 (2006) 131–142.
[14] A.J. Miller, M.C. Mihm Jr., Melanoma, N. Engl. J. Med. 355 (2006) 51–65.
[15] V.I. Alexaki, D. Javelaud, L.C. Van Kempen, K.S. Mohammad, S. Dennler, F. Luciani, K.S. Hoek, P. Juarez, J.S. Goydos, P.J. Fournier, C. Sibon, C. Bertolotto, F. Verrecchia, S. Saule, V. Delmas, R. Ballotti, L. Larue, P. Saiag, T.A. Guise, A. Mauviel, GLI2-mediated melanoma invasion and metastasis, J. Natl. Cancer Inst. 102 (2010) 1148–1159.
[16] Y. Kang, J. Massague, Epithelial-mesenchymal transitions: twist in development and metastasis, Cell 118 (2004) 277–279.
[17] J.P. Thiery, H. Acloque, R.Y. Huang, M.A. Nieto, Epithelial-mesenchymal transitions in development and disease, Cell 139 (2009) 871–890.
[18] L. Kerosuo, M. Bronner-Fraser, What is bad in cancer is good in the embryo: importance of EMT in neural crest development, Semin. Cell Dev. Biol. 23 (2012) 320–332.
[19] B. De Craene, G. Berx, Regulatory networks defining EMT during cancer initiation and progression, Nature reviews, Cancer 13 (2013) 97–110.
[20] H. Yang, L. Wang, J. Zhao, Y. Chen, Z. Lei, X. Liu, W. Xia, L. Guo, H.T. Zhang, TGF-beta-activated SMAD3/4 complex transcriptionally upregulates N-cadherin expression in non-small cell lung cancer, Lung Canc. 87 (2015) 249–257.
[21] T. Tanaka, K. Goto, M. Iino, Sec8 modulates TGF-beta induced EMT by controlling N-cadherin via regulation of Smad3/4, Cell. Signal. 29 (2017) 115–126.
[22] J. Zavadil, E.P. Bottinger, TGF-beta and epithelial-to-mesenchymal transitions, Oncogene 24 (2005) 5764–5774.
[23] A. Moustakas, C.H. Heldin, Signaling networks guiding epithelial-mesenchymal transitions during embryogenesis and cancer progression, Canc. Sci. 98 (2007) 1512–1520.
[24] J. Massague, TGFbeta in cancer, Cell 134 (2008) 215–230.
[25] S. Itoh, F. Itoh, M.J. Goumans, P. Ten Dijke, Signaling of transforming growth factor-beta family members through Smad proteins, Eur. J. Biochem. 267 (2000) 6954–6967.
[26] J. Massague, How cells read TGF-beta signals, Nature reviews, Mol. Cell Biol. 1 (2000) 169–178.
[27] A. Moustakas, S. Souchelnytskyi, C.H. Heldin, Smad regulation in TGF-beta signal transduction, J. Cell Sci. 114 (2001) 4359–4369.
[28] Y. Drabsch, P. ten Dijke, TGF-beta signalling and its role in cancer progression and metastasis, Canc. Metastasis Rev. 31 (2012) 553–568.
[29] K. Giehl, Y. Imamichi, A. Menke, Smad4-independent TGF-beta signaling in tumor cell migration, Cells Tissues Organs 185 (2007) 123–130.
[30] S. Lheureux, K. Karakasis, E.C. Kohn, A.M. Oza, Ovarian cancer treatment: the end of empiricism? Cancer 121 (2015) 3203–3211.
[31] A. Jemal, F. Bray, M.M. Center, J. Ferlay, E. Ward, D. Forman, Global cancer statistics, CA Canc. J. Clin. 61 (2011) 69–90.
[32] B.M. Nolen, A.E. Lokshin, Protein biomarkers of ovarian cancer: the forest and the trees, Future Oncol. 8 (2012) 55–71.
[33] H. Zhang, J. Zhang, Z. Wang, D. Lu, J. Feng, D. Yang, X. Chen, X. Yan, CD146 is a potential marker for the diagnosis of malignancy in cervical and endometrial cancer, Oncol. Lett. 5 (2013) 1189–1194.
[34] Z. Wang, X. Yan, CD146, a multi-functional molecule beyond adhesion, Canc. Lett. 330 (2013) 150–162.
[35] A. Ouhtit, R.L. Gaur, Z.Y. Abd Elmageed, A. Fernando, R. Thouta, A.K. Trappey, M.E. Abdraboh, H.I. El-Sayyad, P. Rao, M.G. Raj, Towards understanding the mode of action of the multifaceted cell adhesion receptor CD146, Biochim. Biophys. Acta 1795 (2009) 130–136.
[36] I.M. Shih, The role of CD146 (Mel-CAM) in biology and pathology, J. Pathol. 189 (1999) 4–11.
[37] G. Zabouo, A.M. Imbert, J. Jacquemier, P. Finetti, T. Moreau, B. Esterni, D. Birnbaum, F. Bertucci, C. Chabannon, CD146 expression is associated with a poor prognosis in human breast tumors and with enhanced motility in breast cancer cell lines, Breast Cancer Res. 11 (2009) R1.
[38] Q. Gao, J. Zhang, X. Wang, Y. Liu, R. He, X. Liu, F. Wang, J. Feng, D. Yang, Z. Wang, A. Meng, X. Yan, The signalling receptor MCAM coordinates apical-basal polarity and planar cell polarity during morphogenesis, Nat. Commun. 8 (2017) 15279.
[39] T. Jiang, J. Zhuang, H. Duan, Y. Luo, Q. Zeng, K. Fan, H. Yan, D. Lu, Z. Ye, J. Hao, J. Feng, D. Yang, X. Yan, CD146 is a coreceptor for VEGFR-2 in tumor angiogenesis, Blood 120 (2012) 2330–2339.
[40] J. Chen, Y. Luo, H. Hui, T. Cai, H. Huang, F. Yang, J. Feng, J. Zhang, X. Yan, CD146 coordinates brain endothelial cell-pericyte communication for blood-brain barrier development, Proc. Natl. Acad. Sci. U. S. A. 114 (2017) E7622–E7631.
[41] Z. Ye, C. Zhang, T. Tu, M. Sun, D. Liu, D. Lu, J. Feng, D. Yang, F. Liu, X. Yan, Wnt5a uses CD146 as a receptor to regulate cell motility and convergent extension, Nat. Commun. 4 (2013) 2803.
[42] R. Derynck, Y. Zhang, X.H. Feng, Smads: transcriptional activators of TGF-beta responses, Cell 95 (1998) 737–740.
[43] R. Derynck, Y.E. Zhang, Smad-dependent and Smad-independent pathways in TGF-beta family signalling, Nature 425 (2003) 577–584.
[44] W. He, D.C. Dorn, H. Erdjument-Bromage, P. Tempst, M.A. Moore, J. Massague, Hematopoiesis controlled by distinct TIF1gamma and Smad4 branches of the TGFbeta pathway, Cell 125 (2006) 929–941.
[45] Q. Zeng, W. Li, D. Lu, Z. Wu, H. Duan, Y. Luo, J. Feng, D. Yang, L. Fu, X. Yan, CD146, an epithelial-mesenchymal transition inducer, is associated with triple-negative breast cancer, Proc. Natl. Acad. Sci. U. S. A. 109 (2012) 1127–1132.
[46] S.H.M. Wong, C.M. Fang, L.H. Chuah, C.O. Leong, S.C. Ngai, E-cadherin: its dysregulation in carcinogenesis and clinical implications, Crit. Rev. Oncol. Hematol.

121 (2018) 11–22.
[47] J. Massague, TGFbeta signalling in context, Nat. Rev. Mol. Cell Biol. 13 (2012) 616–630.
[48] J. Massague, TGF-beta signaling in development and disease, FEBS Lett. 586 (2012) 1833.
[49] X.H. Feng, R. Derynck, Specificity and versatility in tgf-beta signaling through Smads, Annu. Rev. Cell Dev. Biol. 21 (2005) 659–693.
[50] E. Vasilaki, M. Morikawa, D. Koinuma, A. Mizutani, Y. Hirano, S. Ehata, A. Sundqvist, N. Kawasaki, J. Cedervall, A.K. Olsson, H. Aburatani, A. Moustakas, K. Miyazono, C.H. Heldin, Ras and TGF-beta signaling enhance cancer progression by promoting the DeltaNp63 transcriptional program, Sci. Signal. 9 (2016) ra84.
[51] A.K. Perl, P. Wilgenbus, U. Dahl, H. Semb, G. Christofori, A causal role for E-cadherin in the transition from adenoma to carcinoma, Nature 392 (1998) 190–193.
[52] E.Z. Chai, M.K. Shanmugam, F. Arfuso, A. Dharmarajan, C. Wang, A.P. Kumar, R.P. Samy, L.H. Lim, L. Wang, B.C. Goh, K.S. Ahn, K.M. Hui, G. Sethi, Targeting transcription factor STAT3 for cancer prevention and therapy, Pharmacol. Therapeut. 162 (2016) 86–97.
[53] K. Utsugisawa, Y. Nagane, D. Obara, H. Tohgi, Over-expression of alpha7 nicotinic acetylcholine receptor induces sustained ERK phosphorylation and N-cadherin expression in PC12 cells, Brain Res. Mol. Brain Res. 106 (2002) 88–93.
[54] M.T. Lau, W.K. So, P.C. Leung, Fibroblast growth factor 2 induces E-cadherin down-regulation via PI3K/Akt/mTOR and MAPK/ERK signaling in ovarian cancer cells, PLoS One 8 (2013) e59083.
[55] S. Islam, T.E. Carey, G.T. Wolf, M.J. Wheelock, K.R. Johnson, Expression of N-cadherin by human squamous carcinoma cells induces a scattered fibroblastic phenotype with disrupted cell-cell adhesion, J. Cell Biol. 135 (1996) 1643–1654.
[56] S. Nakajima, R. Doi, E. Toyoda, S. Tsuji, M. Wada, M. Koizumi, S.S. Tulachan, D. Ito, K. Kami, T. Mori, Y. Kawaguchi, K. Fujimoto, R. Hosotani, M. Imamura, N-cadherin expression and epithelial-mesenchymal transition in pancreatic carcinoma, Clin. Canc. Res. 10 (2004) 4125–4133.
[57] D. Ciolczyk-Wierzbicka, D. Gil, P. Laidler, The inhibition of cell proliferation using silencing of N-cadherin gene by siRNA process in human melanoma cell lines, Curr. Med. Chem. 19 (2012) 145–151.
[58] M.Y. Hsu, F.E. Meier, M. Nesbit, J.Y. Hsu, P. Van Belle, D.E. Elder, M. Herlyn, E-cadherin expression in melanoma cells restores keratinocyte-mediated growth control and down-regulates expression of invasion-related adhesion receptors, Am. J. Pathol. 156 (2000) 1515–1525.
[59] R.Y. Liu, Y. Zeng, Z. Lei, L. Wang, H. Yang, Z. Liu, J. Zhao, H.T. Zhang, JAK/STAT3 signaling is required for TGF-beta-induced epithelial-mesenchymal transition in lung cancer cells, Int. J. Oncol. 44 (2014) 1643–1651.
[60] K.H. Cho, K.J. Jeong, S.C. Shin, J. Kang, C.G. Park, H.Y. Lee, STAT3 mediates TGF-beta1-induced TWIST1 expression and prostate cancer invasion, Canc. Lett. 336 (2013) 167–173.
[61] B. Ohkawara, K. Shirakabe, J. Hyodo-Miura, R. Matsuo, N. Ueno, K. Matsumoto, H. Shibuya, Role of the TAK1-NLK-STAT3 pathway in TGF-beta-mediated mesoderm induction, Genes Dev. 18 (2004) 381–386.
[62] S. Wang, Y. Cheng, Y. Zheng, Z. He, W. Chen, W. Zhou, C. Duan, C. Zhang, PRKAR1A is a functional tumor suppressor inhibiting ERK/Snail/E-cadherin pathway in lung adenocarcinoma, Sci. Rep. 6 (2016) 39630.
[63] K.K. Velpula, A.A. Rehman, B. Chelluboina, V.R. Dasari, C.S. Gondi, J.S. Rao, K.K. Veeravalli, Glioma stem cell invasion through regulation of the interconnected ERK, integrin alpha6 and N-cadherin signaling pathway, Cell. Signal. 24 (2012) 2076–2084.